Final report for:

Bridge deck slabs with non-metallic reinforcement

Funding from Department of Transport on behalf of the UK Bridges Board

Prepared by: **Dr Su Taylor**
School of Planning Architecture & Civil Engineering QUB

Date: **February 2012 (updated based on comments from BOF)**

For: **The Bridge Owners Forum**

Details of the project are detailed below:

Name of Project	**Thompson's Bridge Replacement**
Name of Structure	**Thompson's Bridge**
Structure Ref No	**60364**

Tender leaders	**Queen's University Belfast**
DRD bridge designers	**Amey Plc**
Contract awarded	**McLaughlin and Harvey with sub-contract design to Aecom, Glasgow**

Contents

1 Project Background and benefits

Recent technological developments in new materials have overtaken current design standards; for example, non-metallic reinforcements such as Fibre Reinforced Polymers (FRPs). Similarly, recent progress in understanding the behaviour of deck slabs (such as membrane effects) are not included in the majority of our current design standards, such as EC2 (BS EN 1992). This project has advanced our understanding and should assist in the development of Standards which promote durable concrete infrastructure taking into account both FRP and Compressive Membrane Action. This project addressed the vitally important area of durable bridge deck construction and offered the chance to investigate an alternative to corrosive steel reinforcement, namely basalt fibre reinforced polymer (BFRP). It provided a unique opportunity for the monitoring of a durable highway structure which will be of benefit to all asset managers of such structures. The development of durable and cost-effective materials is essential to future sustainable development. It is estimated that it costs in excess of £600m on the repair and rehabilitation of concrete infrastructure annually in the UK and a large proportion of this is due to the corrosion of steel reinforcement embedded within the concrete (Parke, 2005). This is not just at the level of millions of pounds for repair, rehabilitation and replacement (Koch et al , 2001) but also for ‘cleaning-up’ the contamination that would inevitably arise from major structural failure. Hence the use of wholly durable, robust yet lightweight polymer reinforcement is of particular benefit to sustainable infrastructure and the outcome of this project has assisted in the acceptance of FRP as internal reinforcement in concrete construction.

Thompson’s bridge is a replacement bridge carrying the A509 in Co. Fermanagh. The bridge was originally designed as a fully integral two-span underbridge, consisting of reinforced concrete abutments on piled foundations, and a reinforced concrete central pier, founded on pile foundations in the river. However, the contractors detailed an engineered alternative consisting of a fully integral single span skew bridge with four ‘W11’ precast pre-stressed beams and a reinforced concrete bridge deck slab. It is anticipated that no maintenance will be required to the new FRP reinforced concrete deck which is of particular importance as this bridge crosses the Upper Cladagh or Swanlinbar River which is home to the freshwater pearl mussel. It is one of the few rivers in Northern Ireland that still retains a significant and viable population of this rare shellfish. In addition, the Atlantic Stream Crayfish, otters and Kingfishers are also present along this length of the river.

The specific benefits of this project

- To development of durable and cost-effective materials for future sustainable development, namely, high performance lower energy concrete and non-metallic corrosion resistant reinforcement (FRPs).
- Understand the behaviour of deck slabs with membrane effects so current design standards can be used to promote the most economical and durable design
- Previous research has highlighted the service behaviour is critical in slabs reinforced with FRP bars but this project showed that compressive membrane has a beneficial influence on the service behaviour and the deflections were lower in the FRP sections than in the equivalent steel reinforced section
- This research advanced the knowledge and understanding of new materials in bridge deck slabs.
- This project should help to promote both durable and economic bridge decks particularly and to advance the understanding decks with non-metallic reinforcement

2 Background to Compressive Membrane Action

In the past 30 years it has become increasingly evident that corrosion of reinforcement due to the effects of de-icing salts has been one of the major factors in the deterioration of reinforced concrete bridge decks (Koch et al, 2000). Detailing to reduce the risk of corrosion is simpler if the percentage of conventional reinforcement is low. If the edges of the slab are restrained against lateral movement by a stiff boundary, an internal arching mechanism or Compressive Membrane Action is induced as the slab deflects. This enhances the flexural load capacity of the slab. The arching phenomenon occurs in concrete due to the significant difference between its tensile and compressive strengths. The weak strength in tension causes cracking due to the application of load. This shifts the neutral axis towards the compression face. If the edges of the slab are restrained by a stiff boundary, internal arching action is induced (Fig.1).

The enhancement in slab strength, due to arching or Compressive Membrane Action (CMA), has been incorporated into some design standards; including the Department of the Environment (NI) (now the Department of Regional Development) 'Design Specification for Bridge Decks' (1990) and more recently the design guidance, BD81/01, 'Use of Compressive Membrane Action in Bridge Deck Slabs'

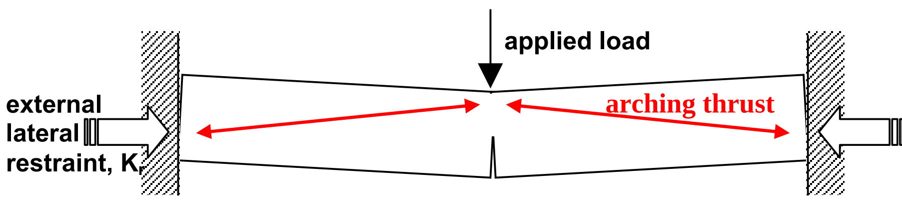

Fig. 1: Compressive membrane action in laterally restrained reinforced concrete slab

The behaviour at low loading is elastic, region A to B in Fig.2, but reaches an elastic-plastic phase, B to C, prior to the peak load at C. This peak load corresponds to the maximum arching effect and, in under reinforced slabs, the maximum bending strength. At increased deflection, the subsequent load capacity reduces.

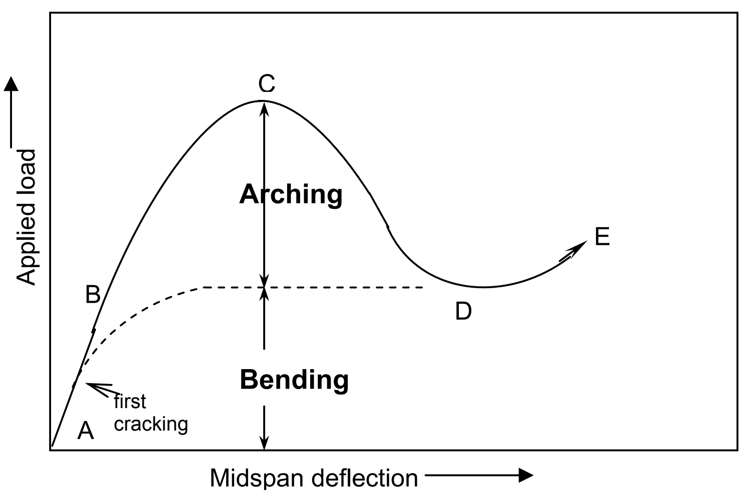

Fig. 2 : Typical load vs. deflection for restrained reinforced concrete slab

It has been shown that the arching effect is relatively greater in slabs with lower reinforcement percentage, low span to depth ratio, high degree of lateral restraint and higher concrete compressive strength. That is, in comparison to the flexural or yield line predicted ultimate strengths which do not consider membrane effects.

2.1 Bridge deck slab design

Global and local behaviour

The global behaviour of a bridge structure is determined by the overall distribution of forces and deflection both longitudinally and transversely. This analysis is normally carried out for a complex envelope of loads representing the many different load combinations which are achievable. The local behaviour is the effect on a particular element of the structure caused by individual loads, for example, a wheel load on a section of the deck slab. In the design, and the assessment, of bridge structures it can be difficult to assess the combined effects of both the local and the global load. Therefore, in most cases, the two effects are treated independently. In the UK, bridge designers combine the worst coexistent local and global load effects and in the design of the deck slab of a beam-and-slab type bridge it is generally the local effects which dominate.

2.2 Design codes

Currently the EU Standard for reinforced concrete bridge design (BS EN 1992), in conjunction with the Departmental Standards BD15/92, BD24/92, BD37/01 and BD44/95 recommends the use of elastic methods to assess the local effects of wheel load. This generally gives a level of transverse reinforcement of between 1.2% and 1.7% in the deck slab. However, this analysis is based upon stiffness matrix method or plate theory assuming a linear elastic material and are not representative of the behaviour of an in-plane restrained reinforced concrete slab which has both material and geometric non-linearity. In other words, the effect of membrane action has been neglected. A detailed programme of field tests in Northern Ireland showed the deck slabs of M-beam type bridges with reinforcement ratios of less than one third of those calculated using the design charts performed satisfactorily. Subsequently the Northern Ireland Standard (DoE (NI), 1990) was amended to reduce the amount of reinforcement. The code suggests the use of 0.6%, top and bottom, transverse reinforcement in the deck slab of M-beam type bridges with a main beam spacing of 2m or less. This includes a fairly high safety margin based upon the results of field tests but halves the amount of reinforcement compared to that predicted by elastic methods.

There are a number of limitations in the use of this standard. The span to depth ratio is restricted to less than 15 and the tests were based on a 160mm deck slab. Following this research at QUB, the Highways Agency has produced the design guidance BD81/01, 'Use of Compressive Membrane Action in Bridge Deck Slabs'. A small number of other countries have adapted their codes to recognise the presence of CMA such as the Canadian Code (CHBDC, 2010).

2.3 Research into CMA at Queen's University Belfast

In the late 1970s the effects of compressive membrane action were being investigated at QUB and have continued until the present day. Rankin (1982) developed a rational approach for the strength of laterally restrained reinforced concrete slabs for use in predicting the strength of two-way spanning slabs under a concentrated load. Kirkpatrick (1984) investigated arching in the deck slabs of M-beam bridge deck slabs. This included both field and laboratory tests. The analysis of punching was developed by modifying the model above. More recent research at QUB into compressive membrane action the effects CMA in high strength concrete bridge deck slabs. The extent of arching action is dependent upon the degree of lateral restraint and this has proved difficult to quantify. Taylor et al (2003) provided a method for assessing the degree of lateral restraint by using a restraint model and this is described more fully in a Guide to the use of CMA (Taylor et al, 2002). This research also investigated novel ways in which the slab could be more effectively and efficiently reinforced. This included the use of polypropylene fibres within the concrete which reduce thermal and shrinkage cracking to further enhance the long term durability. Field tests on the Corick bridge (Taylor et al, 2007) showed that slabs with as low as 0.25%C reinforcement in one layer at mid-depth behaved similarly to 0.6% top and bottom reinforced slabs up to an applied load of 400kN. This work was extended to investigate the use of non-ferrous reinforcement, namely FRP, in the concrete bridge deck slabs (Taylor and Mullin, 2006). The results showed that the FRP reinforced slab had slightly improved service behaviour and higher ultimate capacity than the equivalent steel reinforce slab but this was mainly due to slight difference in the concrete compressive strength. More recently CMA in steel–composite bridge decks slabs has been investigated and modelled numerically using Non Linear Finite Element Analysis (Zheng et al, 2010)

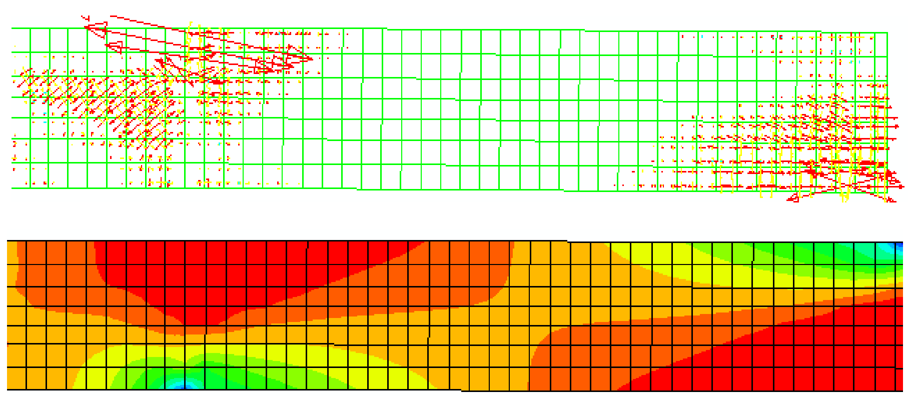

Fig. 3: Crack distribution and CMA in RC Slabs from NLFEA

2.4 Summary of methods for predicting the strength of laterally restrained bridge deck slabs

Comparison to the existing code (BS EN 1991)

In the European Standard and associated BDs, a bridge structure is designed to resist the worst combination traffic loading with other live loads such as wind and temperature. However, as discussed in Section 2, the predominating criterion for the design of the deck slab is the local effect under a concentrated wheel load. The bending capacity can described by the following equation (with the safety factors removed):

$$\mathbf{M_b = A_s.\,\mathit{f}_y.d\,(1 - (0.746A_s.\,\mathit{f}_y/\,\mathit{f}_{cu}.b.d))} \qquad \textbf{[Eqn. 1]}$$

The equation has been used to predict the flexural strength of Taylor et al's (2001) tests on one-way spanning slab strips and test results clearly show an increase in ultimate strength with increasing concrete compressive strength but this is not recognised by the design code (Figure 4). The test results also demonstrated an increase in the ultimate strength with an increase in the in-plane restraint. This is also neglected in the current code methods deck slabs and in reality there is a substantial enhancement in both the flexural and punching shear capacities due to Compressive Membrane Action.

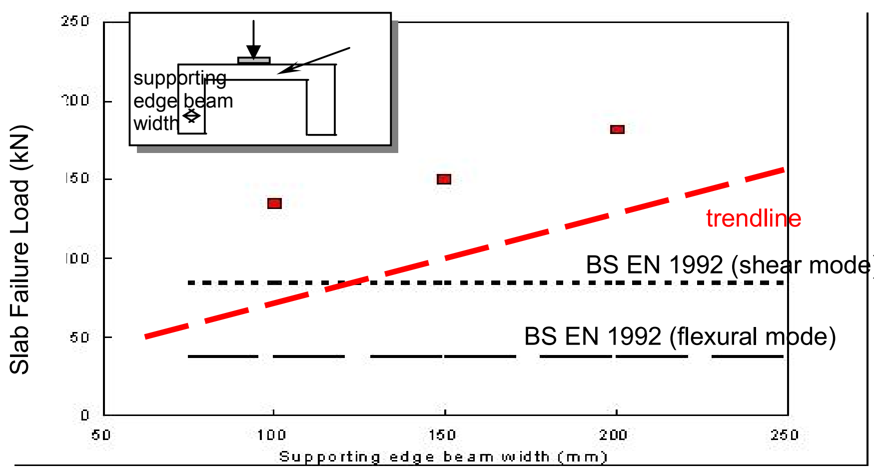

Fig.4: Comparison of 1/3-scale model bridge deck slab failure loads to predicted values in design code

2.4.1 Queen's University of Belfast approach and BD81/02

Arching theory

The arching theory separates the bending and arching components. In reality the two mechanisms are combined and the compression in the concrete is due to both the action of arching and bending. Rankin and Long (1997) extended the theory of McDowell, McKee and Sevin (1956) which focused on the geometry of deformation of laterally restrained masonry walls. Two non-dimensional parameters, R and u, are used to describe the geometry of deformation:

$$R = \frac{\varepsilon_c . L_r^2}{4.d_1^2}. \quad \text{and} \quad u = \frac{w}{2d_1} \qquad \textbf{[Eqn.1]}$$

'R' is a measure of the elastic deformation and 'u' is a non-dimensional measure of the deflection of the slab strip and ε_c is the idealised concrete plastic strain (see Eqn. 4) , L_r, is half the span of the rigidly restrained arch, w is the deflection under the load point (or wheel load) and d_1 is half of the arching depth. Rankin (1982) mathematically manipulated these terms to derive an expression for the arching moment ratio (M_r) where:

(i) R > 0.26: $$\mathbf{M_r = \frac{0.3615}{R} \text{ and } u = 0.31 \text{ (constant)}} \qquad \textbf{[Eqn.2]}$$

(ii) 0 < R < 0.26: $$\mathbf{M_r = 4.3 - 16.1\sqrt{3.3x10^{-4} + .1243R}}$$
$$\mathbf{u = -0.15 + 0.36\sqrt{0.18 + 5.6R}} \qquad \textbf{[Eqn.3]}$$

In predicting the arching strength of restrained reinforced concrete slabs it is, therefore, necessary to establish the depth of the arching section, $2d_1$, and the plastic strain value, ε_c. The depth of section available for arching is firstly estimated from the overall depth minus the depths of the compression zones due to bending. The plastic strain value is the value of strain when full plasticity is first achieved. This was established using an equivalent trapezoidal stress block. The value of the plastic strain is then given as:

$$\boldsymbol{\varepsilon_c = 2\ \varepsilon_u.\ (1-\beta)} \qquad \textbf{[Eqn.4]}$$

$$\boldsymbol{\Rightarrow \varepsilon_c = (-400 + 60f'_c - 0.33f'^2_c)\ 10^{-6}}$$

The strength of laterally restrained slabs is highly dependent upon the degree of external lateral restraint. Therefore, the restrained slab system with finite restraint stiffness was equated to a rigidly restrained slab, i.e. infinite stiffness, using the three-hinged arch analogy as discussed in Section 3.4. The solution to the equilibrium equation is outlined in Appendix B of Rankin's thesis (1982). In summary, the longer equivalent rigidly restrained slab has been used to describe the load-deformation response of a shorter finitely restrained slab.

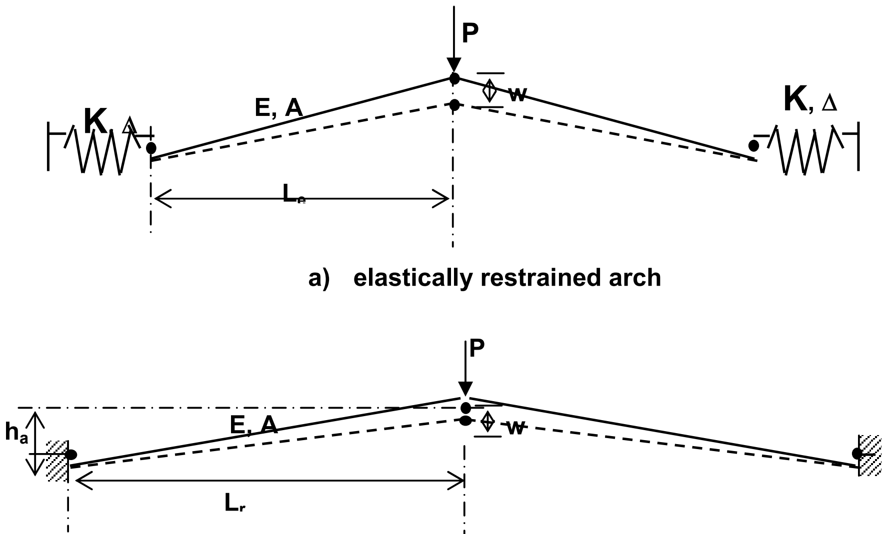

a) elastically restrained arch

b) equivalent rigidly restrained arch

Fig. 5 : Analogy of three-hinged arch

The equivalent length is then given by:

$$L_r = L_e \sqrt[3]{\left(\frac{E_c.A}{KL_e} + 1\right)} \qquad \textbf{[Eqn.5]}$$

This provided a simple analytical expression which could be incorporated into the non-dimensional parameters used to describe arching moment. The stiffness of the slab strip has been based upon the axial stiffness where:

$\mathbf{K = E_cA/L_e}$ where $\mathbf{A = \alpha.\ d_1}$ per unit width, and $\mathbf{E_c = 4.23\ \mathit{f}_{cu}^{\,0.5}}$ **[Eqn.6]**

'A' is the depth of the contact zone as described and the value for the elastic modulus has been based upon Hognestad's relationship. Hence, a means of obtaining the arching moment of resistance for a slab strip with finite lateral restraint had been achieved. However, both the length of the equivalent rigidly restrained strip and the contact area are dependent upon the degree of lateral restraint and this method requires an iterative process to determine a constant value of d_1. The British Standard, BS5400, assumes one value for the ultimate strain and describes the parabolic stress block by an equivalent stress block equal to 0.9x (Fig.10). It has been proven that the value of ultimate strain changes with concrete strength and a report by the Concrete Society (1999) proposed a series of stress-strain relationships for concrete with varying compressive strength up to 115N/mm^2. The stress-strain relationship was used to develop an equivalent rectangular stress block.

Taylor et al (2001) outlined the adaptation to the material properties to incorporate both normal strength concrete (NSC) and high strength concrete (HSC). The variation in the ultimate strain can be represented by the following equation:

$$\varepsilon_u = 0.0043 - [\,(f_{cu} - 60) \cdot 2.5 \times 10^{-5})] \qquad \textbf{[Eqn.7]}$$

The depth of the stress block is also given by:

$$\beta = 1 - 0.003 f_{cu} \qquad \textbf{[Eqn.8]}$$

where β is the depth of the equivalent rectangular stress block as a fraction of the depth of the neutral axis from the compression face.

The method outlined above predicts the enhanced flexural capacity of laterally restrained slab strips but is not directly applicable to the punching strength of bridge deck slabs. A means of assessing the degree of lateral restraint inherent in such a system is critical to the prediction and in the past this has not been achieved satisfactorily. It has been established that the width of the edge beams had a significant influence on the ultimate strength of the slabs tested by the authors. Taylor et al (2003) used a model restraint system where the supporting edge beams, end diaphragms and surrounding area of unloaded slab were equated to a spring of an equivalent stiffness. It was estimated that the influence of the arching force was sufficiently low at a distance equal to the effective span plus the depth of the slab (L_e + h) from the face of the support.

This observation agreed with others' findings, such as those by Fang et al (1994). Initially the value of external lateral restraint stiffness was used in an elastic-plastic method for a two-way spanning slab with the elastic and plastic moment factors ascertained from a finite element analysis and yield line analysis respectively. A simplification to the method to facilitate its use by designers was considered to be of primary importance.

A fundamental simplification in the preceding analytical approach was the assessment of the degree of lateral restraint by a 'restraint model'. This gave reasonable predictions for the strength of the bridge deck models tested and the restraint model provided an adequate basis for a simplified approach. A typical bridge deck restraint model is illustrated in Fig.11 and the method is described in more detail in the Design Guide for the CBDG (Taylor et al, 2002).

The following flow chart illustrates the steps to be taken in the calculation procedure for the flexural and shear punching strengths of laterally restrained slabs.

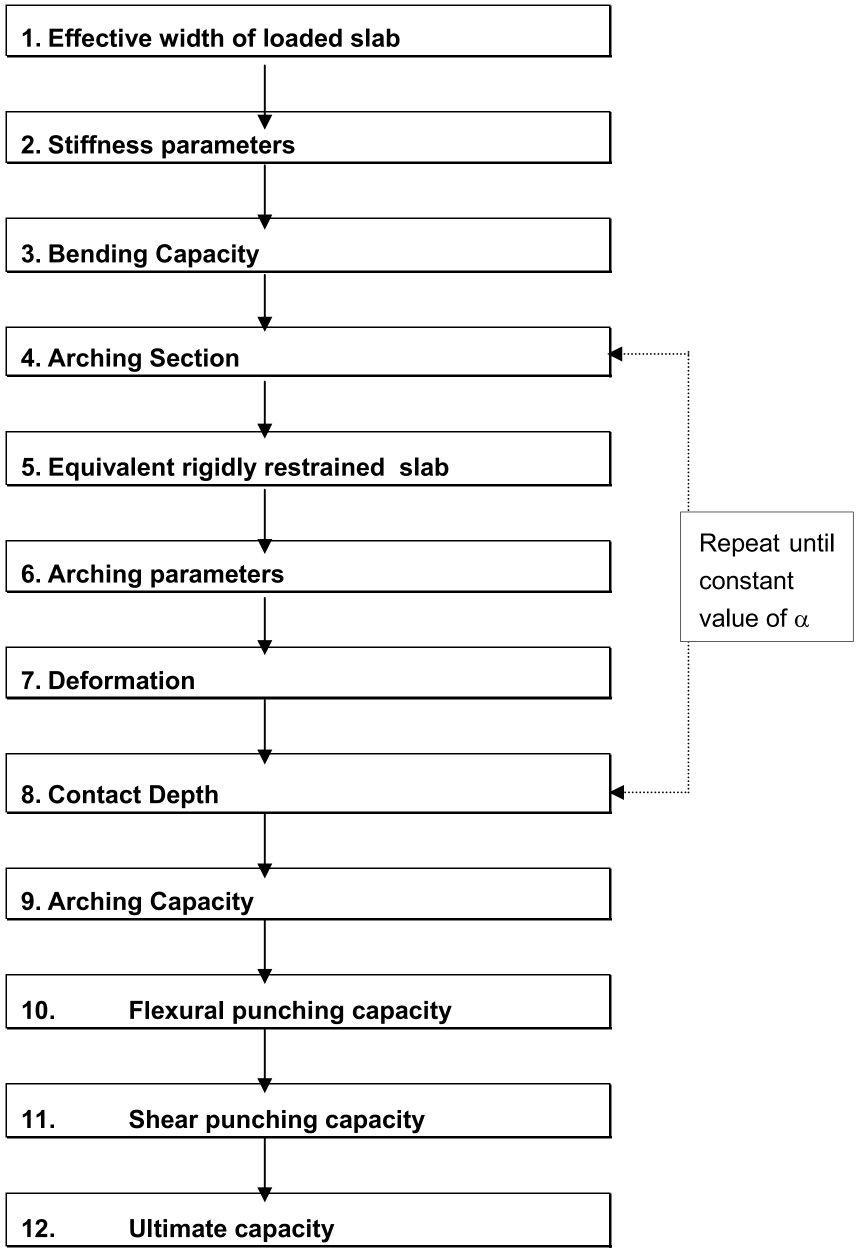

2.4.2 BD81/02 method

This is a simplified method for assessing the enhanced punching capacity of reinforced concrete bridge deck slabs by considering arching action. It assumes that a bridge deck slab has a high in-plane restraint and the mechanism of failure is a punching shear mode. It assumes that the diaphragms provided the necessary restraint to prevent the transverse movement of the beams due to the arching thrust. The design charts were used to establish the maximum arching moment in terms of the concrete compressive strength and the span to depth ratio where:

$$\mathbf{M_{ar} = k.}\boldsymbol{f'_c}\mathbf{.\,h^2} \quad \text{and} \quad \mathbf{k = \frac{0.21}{4}.M_r} \quad (\text{Mr} = 4 \text{ for rigid plastic material}; <4 \text{ for elastic-plastic material}) \qquad \textbf{[Eqn.9]}$$

When the maximum arching moment has been calculated it can be related to the equivalent area of flexural reinforcement, ρ_e, using the following:

$$\rho_e = \frac{k.f'_c.h^2}{240d^2} \qquad \textbf{[Eqn.10]}$$

This was than substituted into Long's (1975) equation for the shear punching strength i.e.: for a circular load:

$$\mathbf{P_{pv} = 1.52.(\phi + d).d.\sqrt{f'_c}.(100\rho_e)^{0.25}} \qquad \textbf{[Eqn.11]}$$

or more generally described by:

$$P_{pv} = \frac{0.43}{r_f}\sqrt{f_{cu}}.(critical \quad perimeter).d(100\rho_e)^{0.25} \qquad \textbf{[Eqn.12]}$$

where r_f, shape factor = 1.0 (circular load) or 1.15 (rectangular load) and critical perimeter is taken at 0.5d from the face of the loaded area.

However the arching capacity cannot exceed the maximum capacity as represented in Fig.7 and by the following equation:

$$\mathbf{M_{a(max)} = 0.67}\boldsymbol{f_{cu}}\mathbf{(h/2)^2 = 0.168}\boldsymbol{f_{cu}}\mathbf{\,h^2} \qquad \textbf{[Eqn.13]}$$

2.5 Summary of CMA

From the summary of the proposed methods for predicting the strength of laterally or in-plane restrained slabs, a primary conclusion is that bridge deck slabs have strengths far in excess of those predicted by conventional design methods which are based upon flexural theory. The use of elastic methods, as recommended by BS EN 1992, underestimates the ultimate strength of laterally restrained bridge deck slabs as they take no account of the in-plane forces set-up as a result of Compressive Membrane Action (CMA). The methods based on arching theory gave more accurate predictions for the strength of a wide range of laterally restrained bridge deck type slabs compared to the current codes. The QUB approach gives more consistent and slightly conservative predictions compared to the highly conservative predictions using the design code. The Departmental Standard, BD81/01, has partly addressed the use of CMA for the design and assessment of bridge deck slabs in the UK, although it does not address some of the limitations to its use such as the boundary restraint and particularly its requirement for intermediate diaphragms. Based upon tests on reinforced concrete bridge deck models, a method for evaluating the level of external restraint stiffness has been established.

3 Background to fibre reinforced polymers and basalt fibre

Fibre reinforced polymers (FRPs) continue to have widespread application in aerospace, automotive, and sports as they offer high performance, light weight and reduced lifecycle costs. This can make them highly attractive for use in bridge structures. Currently, FRPs (glass, GFRP; basalt, BFRP or carbon, CFRP) are applied to retrofitting concrete, retrofitting steel, seismic retrofit of bridge piers, bridge decks for special applications, and internal reinforcement for concrete (Mertz et al, 2003). Some bridges have been built entirely or partially of FRP (O'Connor et al, 2011). FRP can offer the advantages of faster construction time, higher strength, lower weight, and greater environmental durability. The main problem associated with FRP applications is the initial cost and the perceived drawback with lower elastic modulus although this is not an issue when compressive membrane action occurs as the concrete compression properties govern behaviour. Among currently used fibres for FRP, glass fibre can have susceptibility to alkaline conditions although the resin used in the pultrusion process, which surrounds the fibres, tend to be far more resistant. Recent results in Canadian bridges have shown corrosion resistance unlike steel rebar embedded in similar concrete bridge deck slabs which have shown signs of corrosion. Stiffer carbon fibre has the disadvantage of very high cost and anisotropy (Kruckenberg, 1998). Other synpolymeric fibres usually have low elastic modulus compared to steel (Ramakrishnan and Neeraj, 1998) but this is less significant when arching action occurs.

Basalt is one of the most common rocks found in the earth's crust. Russia has unlimited basalt reserves (Artemenko, 2003) and the thirty active quarries have roughly 197 million m^3. In the United States, Washington, Oregon and Idaho have thousands of square miles covered with basalt lava. The Columbia Basalt Plateau, located in this region, has about 100,000 square miles covered with basalt (Parnas et al, 2007). Basalt fibres are made from basalt rock by melting the rock at 1300-1700 °C and spinning the molten liquid (Militky, 1996). The first basalt plants were built in USSR in late 1980s and a patent for basalt fibre production was registered in 1991 in Russia. However, continuous basalt fibre was rarely used until the technology of continuous spinning was adapted. The chemical composition of basalt fibre is similar to that of glass fibres (see Table 3.1). As with glass fibres, the mechanical properties of basalt fibres can be slightly different from different sources, possibly due to slightly different chemical components and processing conditions such as drawing temperature. Tensile strength of basalt fibre tends to increase with increasing drawing temperatures, between 900 and 2900 MPa, for temperatures in the range of 1200~1375 °C. Besides good mechanical properties, basalt has high chemo- and thermal stability, good thermal, electrical and sound insulating properties. Basalt composite pipes can transport corrosive liquids and gases (Van de Velde et al at Belgium http://www.basaltex.com/en/r-d.aspx). The replacement of glass fibre with basalt fibre can reduce the risk of environment pollution like high-toxic metals and oxides, which are produced in glass fibre production (Medvedyev, 2004). Furthermore, basalt fibre has higher stiffness and strength than glass fibre, according to some researchers (e.g. Militky, 1996; Tharmarajah et al, 2011.

Table 3.1 Comparison of Chemical Components between Different Fibres

Chemical composition, %	**Basalt**	**E-Glass**	**S-Glass**
Silicone Dioxide, SiO_2	48.8~51	52-56	64-66
Aluminum Oxide, Al_2O_3	14~15.6	12-16	24-26
Iron Oxide, $FeO+Fe_2O_3$	7.3~13.3	0.05-0.4	0-0.3
Calcium Oxide, CaO	10	16-25	0-0.3
Magnesium Oxide, MgO	6.2~16	0-5	9-11
Sodium Oxide & Potassium Oxide, $Na_2O + K_2O$	1.9~2.2	0-2	0-0.3
Titanium Oxide, TiO2	0.9~1.6	0-0.8	-
Phosphorus oxide, P_2O_5			
manganese oxide, MnO	0.1~0.16		
Fluorides		0-1	
Boron Oxide		5-10	

4 Thompson’s Bridge description

Thompson’s bridge is a replacement bridge carrying a two-way, A-class road, number A509 in Co. Fermanagh. The bridge was originally designed as a fully integral two-span underbridge, consisting of reinforced concrete abutments on piled foundations, and a reinforced concrete central pier, founded on pile foundations in the river. However, the contractors detailed an engineered alternative consisting of a fully integral single span skew bridge. The superstructure comprised four ‘W11’ precast pre-stressed beams with a reinforced concrete slab bridge deck. The mid-span section was constructed with BFRP reinforcement as shown in the attached drawings. The site setting and location is described in the AIP documents, Structure Ref No60364 as approved by the Northern Ireland Department for Regional Development, Roads Service. Aecom were sub-contracted for the design of bridge structure for McLaughlin and Harvey Ltd. who provided the project management for the construction of this bridge. Queen’s University provided the design and specification for the FRP deck and load testing. A copy of the drawings is attached Appendix A.

5 Project Management Procedures

The research project was coordinated and managed by the lead partners Queen’s University and despite the complete change in the design of the bridge and reduced timescale for the manufacture and fixing of the sensors, the project ran to the revised Roads Service time and to budget. Technical input was provided by the electronic and mechanical workshops, in the School of Planning, Architecture and Civil Engineering, for the instrumentation and the test rig. Table 5.1 shows the final programme of work but it does not include the work carried out prior to the tender documents being is used including the initial design and AIP with Amey plc. Aecom Ltd. were sub-contractors to McLaughlin and Harvey Ltd for the design of the bridge and have played a key role in ensuring the successful incorporation of the FRP bars, self-compacting concrete and the sensor network. McLaughlin and Harvey Ltd were the overall project managers for the construction and QUB liaised closely with them. Dr Simon Grattan of Sengenia Ltd, contributed to work packages related to the development, installation and monitoring using discrete fibre optic sensor systems and supporting the partners in the collection of data from the sensor network.

Table 5.1 : Gantt chart for the final programme of work for Thompson's bridge (Start date November 2009 – work on original design and AIP not included in this programme)

Descriptions of Tasks	Q 1	Q2	Q3	Q4**
WP1: Design and evaluation of the FRP concrete deck			M1	
WP2: Specification document and risk assessments				M2
WP3: Purchase of FRP bars, calibration, assembly and protection of specifically designed grating-based optical sensors			M3	
WP4: Installation of FRP bars and deck pour in SCC				M4
WP5: Set-up of the instrumentation and test rig				M5
WP6: Load testing and data acquisition				M6
WP7: Analysis of initial test data and reporting				M7
WP8: Longer-term monitoring				M8
** WP8 runs form quarter 4 to 8.				

Milestones	M1: Final design of the FRP deck slab and NLFEA
	M2: Finalised contract documents including relevant specifications and risk assessment for testing
	M3: provision of an efficient and well-calibrated grating-based multi-parameter sensor network ready for evaluation of the FRP reinforced bridge deck and progress report to Dft
	M4: Construction of a highly durable instrumented FRP bridge deck slab
	M5: Fully functioning sensors network and test rig.
	M6: Complete load tests and data acquisition.
	M7: Report on the findings from the initial load test.
	M8: Continued structural health monitoring of Thomson's bridge and final report to be submitted at the end of the second year (1st November 2011)

McLaughlin and Harvey / Aecom

Queen's University Belfast (QUB)

Sengenia Ltd

☆ Progress meetings

▲ Milestone

6 Summary of Programme of Work completed

This project was used to advance the knowledge and understanding of novel, durable materials in bridge deck slabs. The *key objectives* of this project were to promote both durable and economic bridge decks particularly with respect to the whole life performance and to advance the understanding of Compressive Membrane Action in decks with non-metallic reinforcement. The completed work packages are summarised below.

6.1 Workpackage 1 (WP1): Design and evaluation of the FRP concrete deck

WP1 was focused on the NLFEA analysis and arching action theory for the design of the bridge deck slab with FRP rebar. A design of the deck slab was carried out using Highway Agency BD81/02 department standard but with FRP properties. A nonlinear finite element analysis was also completed by QUB. The original design and AIP was completed in November 2008 but an engineering alternative was put forward by the Contractors following contract award. The new design has been completed by Aecom (Glasgow office) in conjunction with QUB and the revised design of the deck was incorporated into the overall analysis (see the attached reinforcement drawings of the final bridge deck in Appendix A).

6.2 Workpackage 2 (WP2): Specification document and risk assessments

WP2 ensured that all aspects of the FRP and low-energy self compacting concrete (SCC) were included in the Contract specification documents. A copy of these included with the AIP documents. This included method statements and risk assessment for all aspects of the project. The original design and specification for FRP, SCC and testing procedures were included in the tender documents and the contract was awarded to McLaughlin and Harvey in 2009. The contractor proposed an engineered alternative and the risk assessments and specifications were subsequently updated for the new skew bridge design and are attached in Appendix B.

6.3 Workpackage 3 (WP3): Purchase of FRP bars, calibration, assembly and protection of specifically designed grating-based optical sensors

WP3 focused on the assembly of the optical sensors using fibre grating-based (FBG) multi-sensor network and Figure 6 shows the workings of an FBG sensor. As the sensors use light waves for measurement, multiple sensors can be placed on one cable and in this case each optical cable had 5 FBG's to give a strain profile along the bar. The technical approach was to integrate all of the sensor probes into a single network, which was illuminated by the broadband source and interrogated by the Fabry-Perot filter. The main deliverable was an efficient and well-calibrated grating-based multi-parameter sensor network for the evaluation of the internally reinforced FRP bridge deck.

Figure 6: Workings of an FBG (Grattan et al. 2006)

For the tender based design the amount and size of the FRP bars was established at the tender stage. The position of the sensors was also detailed at the time of tender which allowed five months for the fabrication of coated FBG sensors for each rebar.

However, the redesigned bridge deck slab was only completed by May 2010 and the finalised rebar schedule issues at the end of May 2010. This left considerably less time for purchasing the bars and fabrication of the sensors for the correct positions on the bars. The fully recoated sensors were not achievable in this new time scale. To ensure that the contract timescale was not affected, the bare sensors were fabricated for each cable and the protection of the specially designed grating based optical sensors was carried out after attaching to the rebar by recoating. This was not the ideal form of protection for use on site (see Fig. 7) and would recommend allowing sufficient time in the contract documents to allow for the fabrication of the recoated sensors from the point of final design not from the Award of Contract. In this contract, the time scale for the demolition of the existing bridge was critical due to salmon spawning in the River in October and QUB compromised on the fabrication time to assist with the contract timeframe.

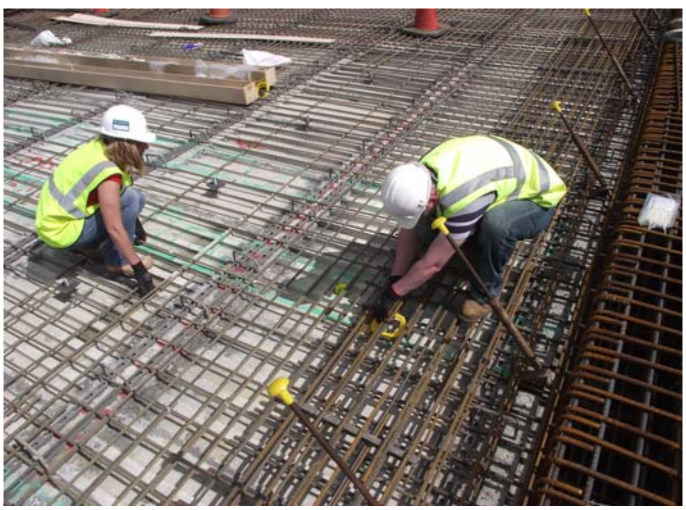

Figure 7: Rebar with optical sensors

However, this did cause delays in handling and fixing on site to avoid damage to the sensors. Several quotes for FRP rebars were obtained and the knowledge gained from a recently completed PhD research project using different FRP rebars was also used in finalising the FRP bar (Thamarajah, 2011). The BFRP bars from Magmatech Ltd. were more durable, highest strength and cost effective choice. Table 6.1 shows the material properties based on tests on control samples of bars using an accurately calibrated direct tensile testing machine with the appropriate load cell. The difference in the values obtained for the tests at QUB compared to the Manufacturer's reported values was the loading rate and the lower value was used in the design calculations with a material factor of safety of 1.5.

Table 6.1 – BFRP and steel material properties

Rebar	Tensile Tests loading rate 0.2kN/s			Manufacturer's reported values loading rate 1kN/s		
	Tensile Strength (MPa)	Elastic Modulus (GPa)	Ultimate Strain µε	Tensile Strength (MPa)	Elastic Modulus (GPa)	Ultimate Strain µS
12mm BFRP	920.0	54.0	17037	1200	50.0	24000
12mm steel	510	210		-	-	-

6.4 Workpackage 4 (WP4): Installation of FRP bars and deck pour in SCC

WP4 ensured the accurate installation of the FRP bars with the sensors and the completion of the deck in lower energy self-compacting concrete to the threshold values specified in the contract documents. The SCC was developed by Tracey Concrete and the mix design is shown in Table 6.2. The suitability of the concrete was determined by slump flow, V-funnel and J-ring tests, in accordance with current EU standards, on site prior to casting of the full deck. McLaughlin and Harvey Ltd revised the AIP in conjunction with the designers Aecom and the attached documents detail the installation and handling of the FRP bars.

Table 6.2: Design mix for Self Compacting Concrete

Material	Quantity (per m^3 concrete)
CEM II (Quinn Cement)	400kg
Limestone Powder (Omya)	250kg
Coarse sand (Loughdoo Aggregates)	713kg
14mm stone (Clarke's)	555kg
10mm stone (Clarke's)	317kg
Chyrso SCC Admixture - polycarboxylate (Chemtec)	4.5 litres

The density of the 12mm BFRP bars is 2250kg/m^3, that is over three times less than that of steel, which means that more bars can be lifted in one bundle compared to steel. If the maximum lift weight is 25kg for 12mm diameter bar by 5m long 19 BFRP bars can be lifted at once compared to 5 bars of the equivalent size in steel. This should equate to more efficient time fixing. Concrete spacers would probably be better for future build using BFRP reinforcement.

Another significant difference in handling the 5m and 6m BFRP rebars was their flexibility compared to steel rebars but this flexibility meant that the bars were more prone to deflect under foot and more spacers blocks were needed than for the steel rebar. This could be overcome in subsequent designs by specifying structural spacers. Another problem was the non-metallic tying wire as the one originally purchased by the contractor was not strong enough which meant increased number of tie positions and more labour time. For future contracts a structural non-metallic tie wire with a minimum strength capability should be specified at tender stage.

6.5 Workpackage 5 (WP5): Set-up of the instrumentation and test

WP5 involved the sensor system set-up for monitoring during load testing and the installation of the self-straining test rig. McLaughlin and Harvey Ltd provided a full platform for safe access to each test area under the deck. The test rig was designed to accommodate the new W-beam deck and the details are covered in the Test report ('Load Test report for Thompson's Bridge', 15th September 2010)

6.6 Workpackage 6 (WP6): Load testing and data acquisition

WP6 was the incremental load testing of various panels within the bridge deck to assess the structural capability of the FRP in comparison to steel as outline in the test report. The *deliverables* were the completed load test and successful data acquisition as outline the test report. Each test panel was loaded to approximately three times the current EU wheel load whilst maintaining a limit on the overall deflection to ensure the load was within the service range of the bridge deck.

6.7 Workpackage 7 (WP7): Analysis of the initial test data and reporting

WP7 completed the analysis of the test data as outline in the test report. The maximum strains and deflections were very low and the FRP reinforced section showed marginally better service performance than the equivalent steel reinforced section. However, this could have been due to minor differences in the effective depth of the rebar and/or slight differences concrete compressive strength causing more membrane action in the FRP section. The strains were comparable to the results from the NLFEA and very low in compariuson to the lower rupture strength of the BFRP.

6.8 Workpackage 8 (WP8): Longer-term monitoring

WP8 was to focus on the longer-term monitoring using the embedded optical sensor network. The strain readings were taken again in Jan 2011 but due to delays on site for Sengenia, at the time of casting concrete and prior to load testing, the sub-contract costs for this were fully utilised. The original programme showed monitoring through the second year with completion by November 2011.

7 Risk Analysis

The principles of M_o_R were applied in the management of risk. Risks were identified, assessed and categorised for each aspect of the project including:

1. Designer’s safety analysis
2. Transportation, handling and fixing of the FRP bars
3. Set-up of the instrumentation
4. Load testing and monitoring

The risk assessments/specification for the the FRP bars and the load testing are attached.

8 Project Costs

The projects costs and claims were processed by the Queen's University Accounting Services. A summary of the breakdown of the claims was reported in the update reports to the Bridge Owners forum and the final costs are shown below. It should be noted that there was a delay in the claims for some of the Work Packages due to changes in key dates, such as the tender award and the change in the design of the bridge. It can be seen that there was a small under spend on the travel costs. The end date was October 2011 but this could be extended if further long-term monitoring can be funded.

QUB Internal Budget (based on revised budget to cover 100% of DI costs)

		Budget £	***final costs £***
DI	Salary	9,114.00	9,114.00
	Travel	3,500.00	3185.66
	Other Costs (incl. material, sub-contract work & Amey design check)	36,525.00	36,588.16
	Equipment	24,350.00	24,203.23
Exceptions	Exceptions	-	-
DA	Investigators	6,358.00	6,359
	Estates	1,719.02	1,719
Indirect	Indirect	23,404.98	23,404
			-
		104,971	**104,573.05**

9 Whole life performance and costing

Current software used to predict life cycle costing and performance are based upon concrete reinforced with corrodible steel bars. One of the major aims of this project was to replace steel rebar with corrosion resistant material, namely basalt fibre reinforced polymer bars. The costings below compare the differences in the construction costs and an anticipated 50 year cost based upon maintenance of an equivalent steel reinforced deck. The rebar costs have been based on 476 no. 6m length 12mm bars and 298 No. 5m length 12mm bars as used in Thompsons bridge. It can also be seen in Figure 8 that the probability of bridge failure increases substantially with increased deterioration, such as that could occur due to corrosion of steel rebar.

	BRIDGE 1 FRP deck	**BRIDGE 1 Steel RC deck**
Rebar costs for (all other costs similar)	£11,697	£4,859.87
Typical maintenance costs and repair at 50 years	£0	At least £50k*
TOTAL difference	£11,697	At least £54,859.87

- estimate based on Stewart (2001) and Canning (2011) and deck panel repairs cost an estimated £250,000 on Hammersmith bridge due to steel corrosion (London Borough of Hammersmith & Fulham, 2011)

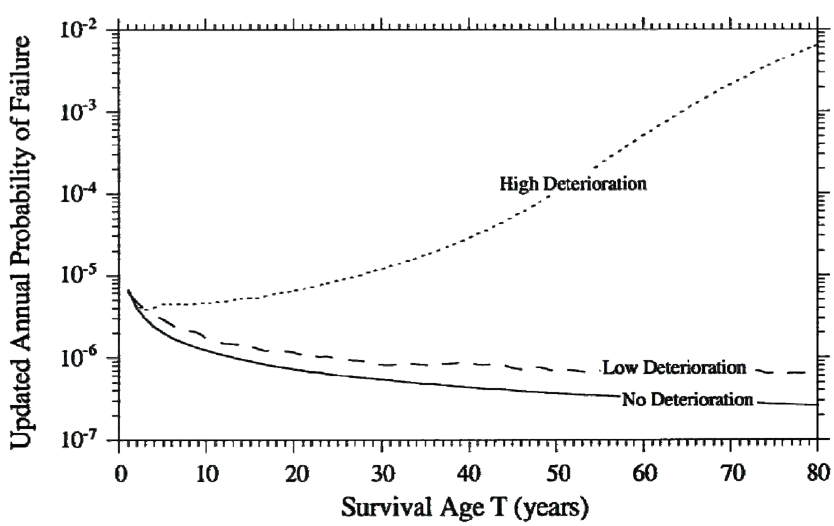

Figure 8 : Comparison of updated annual probabilities of failure (Stewart and Val, 1999)

10 Summary and conclusions

This bridge enabled the first demonstration of non-metallic and corrosion resistant reinforcement in a concrete bridge deck slab in the UK. The primary aim was to show that FRP can be used in combination with inherent arching action to provide a corrosion resistant alternative to steel rebar in reinforced concrete slabs. The recent closure of the Hammersmith Bridge was due to corrosion damaged steel in the concrete deck. The deck panel repairs cost an estimated £250,000 (London Borough of Hammersmith & Fulham, 2011) and this figure does not take into account the associated costs due to disruption and traffic delays. The aim of this project was to produce a maintenance free concrete bridge deck slab and to use structural health monitoring to prove structural performance. Previous research (Tharmarajah, 2011) over the last four years has demonstrated the benefits of BFRP. Basalt fibres have slightly better durability performance compared with E-glass fibres but both types are far more corrosion resistant than steel.

From the design, construction and monitoring of Thompson's bridge deck slab, it can be concluded that the BFRP reinforced concrete bridge deck slab exhibited similar but slightly better structural performance than the equivalent steel reinforced concrete bridge deck slab sections. The deck slab was capable of supporting a wheel load of 40t with no detrimental effect and the maximum test load of 40t was nearly three times the current maximum European wheel load. At 40t, the measured strain values were ~10% of the rupture strain value of the BFRP bars. That is, within the very low service load range. The BFRP test regions also showed good recovery in deflection and strain after unloading.

The maximum deflection in the BFRP slab was 0.78mm at an applied load of 40t and is equivalent to (effective span / 2054) which is well within acceptable limits for deflection. The maximum deflection occurred at the mid-span and there was good recovery in deflection after the removal of all load. The strain values were very low and 8.5 times less than the rupture strain of the BFRP bars at the artificially high applied load of 40t. Strain readings also indicated very low levels of strain in the BFRP bars under live loading and less than those experienced in the load test.

The redesigned bridge deck slab was completed in May 2010 and the finalised rebar schedule issues at the end of May 2010. This left considerably less time for purchasing the BFRP bars and fabrication of the sensors at the correct positions on the transverse slab. The fully recoated sensors were not achievable in this new time scale and this was not the ideal form of protection for use on site. It is recommended to ensure sufficient time, in any future bridges with structural health monitoring, to enable the fabrication of robust sensors from the point of final design and not from the Award of Contract.

The BFRP bars were far lighter than the equivalent sized steel bar enabling easier lifting and handling but the BFRP are also more flexible and require suitable spacers and tie wire and this should be included in the contract documentation at tender stage.

Notation

A	cross sectional area
A_s	area steel reinforcement
E_c	concrete elastic modulus
K	axial stiffness
L_e	half the span of the arch length
L_r	half the span of the equivalent rigidly restrained arch
M_a	arching moment of resistance
$M_{a(max)}$	maximum possible arching moment of resistance
M_{ar}	arching moment of resistance of rigidly restrained slab strip
M_b	flexural moment of resistance at principal section
M_{bal}	balanced moment of resistance
M_r	moment ratio (non-dimensional)
P	applied load
P_a	predicted ultimate arching capacity
P_b	predicted ultimate flexural capacity
R	McDowell's non-dimensional parameter (elastic deformation)
T	tensile force in reinforcement
b	width of section
b_{eff}	effective width of loaded slab
b_o	critical perimeter
c	width of square patch load
c_x	width of patch load parallel to slab span
c_y	width of patch load perpendicular to slab span
d	effective depth of tensile rebar in the slab
d_1	half the arching depth
f'_c	concrete cylinder compressive strength
f_{cu}	concrete compressive strength
f_y	reinforcement yield strength
h	depth of slab
h^*_a	arch height
h_a	arch height
k	arching moment coefficient
r_f	shape factor
s_c	McDowell's maximum compressive stress
u	McDowell's non-dimensional parameter (deflection)
x	depth of concrete compression zone
α	proportion of d_1 in contact with the support
β	proportional depth of stress block (=0.9 in BS)
δ	deflection under the load point
ε_c	concrete compressive plastic strain value
ε_u	concrete maximum compressive strain
γ_M	partial safety factor for strength
ϕ	width of circular patch load
ρ	reinforcement ratio at principal section
ρ_e	effective reinforcement ratio at principal section
ρ_a	effective arching reinforcement ratio at principal section

References/ bibliography

Artemenko, S.E., *Polymer Composite Materials Made From Carbon, Basalt, And Glass Fibres.* Structure and Properties. Fibre Chemistry, 2003. 35(3): p. 226-229.

BD15/92, Departmental Standard, *General principles for the design of and construction of bridges.* Use of BS5400: Part 1: 1988, Highways Agency, December, 1992.

BD24/92, Departmental Standard, *The design of concrete highway bridges and Structures. Use of BS5400: Part 4: 1990*, Highways Agency, December, 1992.

BD37/01, Departmental Standard, *Loads for Highway Bridges, (Supersedes BS5400: Part 2)* Highways Agency, August, 2001.

BD44/95, Departmental Standard, *The assessment of concrete highway bridges*, Department of Transport, Highway and Traffic, January, 1995.

BD81/02, Departmental Standard, *Use of Compressive Membrane Action in bridge decks*, Highways Agency, Nov. 2001.

British Standards Institute, BS EN 1991-2 (2003) *Eurocode 1: Actions on structures —Part 2: Traffic loads on bridges*, European Standard, BSI, London, 2003

British Standards Institute, BS EN 1992 (2004) *Eurocode 2: Design of concrete structures —Part 1-1: General rules and rules for buildings,* European Standard, BSI, London, 2004

Canadian Standards Association (2010), *Canadian Highway Bridge Design Code* CAN/CSA-S6-06 Toronto, Ontario, Canada, 2010, 1078p

Canning, L. *Ministerley Bridge Strengthening Using Novel Methods*, Proceedings of the International conference on Advanced Composites in Construction, UK, 2011

Department of the Environment (NI) *Design Specification for Bridge Decks*, DOE, Northern Ireland, 1990.

Eds. S Liu, G R Edwards, W Hanzalek, D L Olson and C Smith. *International Workshop on Corrosion Control for Marine Structures and Pipelines*. February 9-11, 1999, American Bureau of Shipping

Grattan S K T, Taylor SE , Basheer M , Grattan K, Sun T and Gebremichael y (2006) *Novel Fibre Optic Sensors for Monitoring of Bridges*, Proceedings of Bridge Engineering in Ireland Conference BEI06, December 2006

Jackson P .A. (1990) The global and local behaviour of bridge deck slabs. The Structural Engineer, vol. 68, no. 6,20 March 1990, pp. 112- 116.

Kirkpatrick J., Rankin G.I.B. and Long A.E. (1984) Strength evaluation of M-beam bridge deck slabs. The Structural Engineer, vol. 62B, no. 2, September 1984, pp. 60-67.

Kirkpatrick J., Rankin G.I.B. and Long A.E. (1986) The influence of compressive membrane action on the serviceability of beam and slab bridge decks. The Structural Engineer, vol. 64B, no. 1, March 1986, pp. 6-12.

Koch, G. H., Brongers, M. P., Thompson, N. G., and Payer, J. H. (2001)., *Corrosion Costs and Preventive Strategies In the United States - Report by CC Technologies Laboratories, Inc,* Federal Highway Administration (FHWA) Office of Infrastructure Research and Development, Washington*, D.C.*

Kruckenberg, T.P., Resin transfer moulding for Aerospace Structures (1998) Dordrecht, The Netherlands: Kluwer Academic Publishers.

London Borough of Hammersmith & Fulham Cabinet meeting, 20 JUNE 2011, Agenda Item 9

McDowell, E.L., MvKee, K.E. and Sevin,E (1956), *Arching action theory of restrained masonry walls,* ASCE Journal of Structural Engineering, Vol.82, No.ST2, 1956, pp 915-1– 915-18

Medvedyev, O.O.T., (2004) , *The Outlook for the use of basalt continuous fibres forcomposite reinforcemen*t. International SAMPE Symposium and Exhibition, 2004, 49: p. 2299-2303.

Mertz, D.R., Chajes, M. J. and Gillespie, J. W.,(2003) *Application of Fibre Reinforced Polymer Composites to the Highway Infrastructure*. NCHRP Report 503, Washington DC, USA.

Militky, J.K., Vladimir, (1996) Ultimate Mechanical Properties of Basalt Filaments. TextileResearch Journal,. 66(4): p. 225-229.

Mufti A.A., Jaeger L.G., Bahkt B. and Wegner L.D. (1993) Experimental investigation of fibre reinforced concrete deck slabs without internal steel reinforcement. Canadian Journal of Civil Engineering, vol. 20, 1993.

O'Connor, J Alamplali, S Aref A and Trianafilou L (2011) Strategic Development and Deployment of a Composite Bridge Deck, Proceedings of the International conference on Advanced Composites in Construction, UK, 2011

Parke G, (2005) *Proceedings of Bridge Management*, Fifth International Conference on Bridge Management, University of Surrey, April 2005.

Parnas R , Shaw M, Liu Q, (2007) Basalt Fibre Reinforced Polymer Composites, The New England Transportation Consortium, August, 2007 (NETCR63 Project No. 03-7)

Ramakrishnan, V.T. and Neeraj S., (1998) Performance Evaluation of 3-D Basalt Fibre Reinforced Concrete & Basalt Rod Reinforced Concrete. November USA Transportation Research Board, National Research Council.

Rankin, G.I.B. (1982), Punching failure and compressive membrane action in reinforced concrete slabs, PhD thesis, Queen's University of Belfast, 1982

Rankin, G.I.B. and Long, A.E. (1997), *Arching action strength enhancement in laterally restrained slab strips*, ICE Proceedings – Structures and Buildings, No. 122, Nov. 1997, pp461-467.

Reliability-based assessment of ageing bridges using risk ranking and life cycle cost decision analyses Original Research Article

Stewart M.G., *Reliability Engineering & System Safety*, Volume 74, Issue 3, December 2001, Pages 263-273

Stewart M.G. and Val D. (1999) *Role of load history in reliability-based decision analysis of ageing bridges.* Journal of Structural Engineering, ASCE V.125 N.7 pp776.

Taylor, S.E., Rankin, G.I.B. and Cleland, D.J, (2007) *Membrane action on the serviceability of bridge deck slabs* ACI Structural Journal, V. 104, No. 1, January-February, 2007, pp. 39 – 48.

Taylor, S.E., Rankin, G.I.B. and Cleland, D.J, D.J. (2001) Arching action in high strength concrete slabs, Proceedings of the Institution of Civil Engineers, Structures and Buildings, Vol.146, Issue 4, Nov. 2001 pp.353-362.

Taylor, S.E., Rankin, G.I.B. and Cleland, D.J., (2002) Guide to compressive membrane action in bridge deck slabs, UK Concrete Bridge Development Group/British Cement Association, Technical Paper 3, June 2002.

Taylor, S.E., Rankin, G.I.B. and Cleland, D.J, (2003) High performance concrete bridge deck slabs, Proceedings of the Institution of Civil Engineers, Bridge Engineering, Vol.156, Issue BE2, June 2003 pp.81-90.

Taylor Susan, and Mullin, Barry (2006) Arching action in FRP reinforced concrete slabs, International Journal of Construction and Building Materials Volume 20,

Taylor SE, Gupta A, Robinson D, Grattan S and Long AE (2008), *Monitoring Of Monkstown Bridge*, Proceedings of Structural Faults and Repairs, 2008.

Taylor, S.E., Rankin, G.I.B. and Cleland, D.J, (2007) *Serviceability of bridge deck slabs with arching action* ACI Structural Journal Vol 104 (1) (39-48) DOI

Tharmarajah G., (2011) *Compressive membrane action in fibre reinforced polymer (FRP) reinforced concrete slabs,* PhD thesis, Queen's University Belfast, 2011.

Tharmarajah G., Taylor SE, Robinson D & Cleland DJ (2010) *Composite Reinforcement For Bridge Deck Slabs,* Proceedings of the 8th International conference on Composites in Civil Engineering, IIFC Conference, Beijing, China, Sep. 2010

Van de Velde K., K.P., Van Langenhove L., *Basalt Fibres As Reinforcement For Composites,* University of Ghent, Belgium http://www.basaltex.com/en/r-d.aspx

Zheng Yu, Taylor Su, Robinson Des (2010) *Prediction methods of loading carrying capacities of concrete bridge deck slabs with consideration of Compressive Membrane Action,* Harbin Institute of Technology, Vol.42 No. 4, pp. 1569-1576.

APPENDIX A: Drawings

APPENDIX B: Risk Assessments